

Dalton Transactions

An international journal of inorganic chemistry

Accepted Manuscript

This article can be cited before page numbers have been issued, to do this please use: P. Sun, D. Yang, Y. Li, B. Wang and J. Qu, *Dalton Trans.*, 2020, DOI: 10.1039/C9DT04493K.



This is an Accepted Manuscript, which has been through the Royal Society of Chemistry peer review process and has been accepted for publication.

Accepted Manuscripts are published online shortly after acceptance, before technical editing, formatting and proof reading. Using this free service, authors can make their results available to the community, in citable form, before we publish the edited article. We will replace this Accepted Manuscript with the edited and formatted Advance Article as soon as it is available.

You can find more information about Accepted Manuscripts in the [Information for Authors](#).

Please note that technical editing may introduce minor changes to the text and/or graphics, which may alter content. The journal's standard [Terms & Conditions](#) and the [Ethical guidelines](#) still apply. In no event shall the Royal Society of Chemistry be held responsible for any errors or omissions in this Accepted Manuscript or any consequences arising from the use of any information it contains.

A bioinspired thiolate-bridged dinickel complex with a pendant amine: synthesis, structure and electrocatalytic properties

Received 22th November 2019,
Accepted 00th January 2020

Puhua Sun,^a Dawei Yang,^{*a} Ying Li,^a Baomin Wang^a and Jingping Qu^{*ab}

DOI: 10.1039/x0xx00000x

www.rsc.org/

By employing $X(\text{CH}_2\text{CH}_2\text{S}^-)_2$ ($X = \text{S}$, tpdt; $X = \text{O}$, opdt; $X = \text{NPh}$, npdt) as bridging ligands, four thiolate-bridged dinickel complexes supported by phosphine ligands, $[(\text{dppe})\text{Ni}(\mu\text{-}1, \kappa^2\text{SSS}'\text{:}2, \kappa^2\text{SS-tpdt})\text{Ni}(\text{dppe})][\text{PF}_6]_2$ (**1**)[PF_6]₂, $\text{dppe} = \text{Ph}_2\text{P}(\text{CH}_2)_2\text{PPh}_2$), $[(\text{dppe})\text{Ni}(\mu\text{-}1, \kappa^2\text{SS:}2, \kappa^2\text{SS-npdt})\text{Ni}(\text{dppe})][\text{PF}_6]_2$ (**2**)[PF_6]₂ and $[(\text{dppe})\text{Ni}(\mu\text{-}t\text{-Cl})(\mu\text{-}1, \kappa^2\text{SSX:}2, \kappa^2\text{SS-C}_4\text{H}_8\text{S}_2\text{X})\text{Ni}(\text{dppe})][\text{PF}_6]$ (**3**)[PF_6], $X = \text{S}$; **4**)[PF_6], $X = \text{O}$) were readily obtained by the salt metathesis reaction. These four thiolate-bridged dinickel complexes have all been fully characterized by spectroscopic methods and X-ray crystallography. In **2**)[PF_6]₂, elongation of the Ni–N bond distance, possibly caused by steric hindrance, indicates that the pendant nitrogen group shuttles between the two nickel centers in solution, which is evidenced by $^{31}\text{P}\{^1\text{H}\}$ NMR spectroscopic results. Furthermore, these thiolate-bridged dinickel complexes have all been proved to be electrocatalysts for proton reduction to hydrogen. Notably, complex **2**)[PF_6]₂ featuring a pendant amine group in the secondary coordination sphere exhibits the best catalytic activity at relatively low overpotential.

Introduction

Hydrogen generation has attracted considerable attention, particularly since hydrogen is a clean and sustainable energy carrier when it is derived from proton reduction, which is commonly regarded as a promising alternative to increasingly exhausted fossil fuels.¹ To overcome the major barrier of conversion chemical energy such as H–H bond of hydrogen and electricity for the storage and utilization of energy, much effort has been devoted to the development of active catalysts for hydrogen production during the past decades.² In nature, hydrogenases can effectively catalyze the reversible reduction of protons to release hydrogen under ambient conditions using earth-abundant iron and nickel as active centres.³ Inspired by biological systems, versatile thiolate-bridged diiron and iron-nickel complexes as structural and functional models were designed and synthesized.⁴ However, these biomimetic bimetallic model complexes usually exhibit relatively low turnover frequency (TOF) toward proton reduction to hydrogen compared with some mononuclear nickel complexes.⁵ That is because these mononuclear nickel complexes commonly possess one or more pendant amine groups, which can play as proton relays for

^aState Key Laboratory of Fine Chemicals, Dalian University of Technology, 2 Linggong Road, Dalian, 116024, P.R. China.

^bKey Laboratory for Advanced Materials, East China University of Science and Technology, Shanghai, 200237, P.R. China.

Email: qujp@dlut.edu.cn

yangdw@dlut.edu.cn

Electronic Supplementary Information (ESI) available: Experiment section, spectra and crystal structures. CCDC 1899923–1899925, 1476294. For ESI and crystallographic data in CIF or other electronic format See DOI:10.1039/x0xx00000x

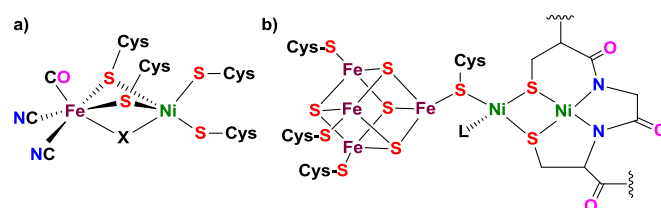


Fig. 1 Structures of active sites of [NiFe]-hydrogenase (a) and acetyl coenzyme A synthase (b).

high catalytic activity similar to the function of the secondary coordination sphere of [FeFe]-hydrogenase.³ For example, Helm *et al.* reported a synthetic mononuclear nickel electrocatalyst supported by $\text{P}^{\text{Ph}}_2\text{N}^{\text{Ph}}$ ($\text{P}^{\text{Ph}}_2\text{N}^{\text{Ph}} = 1,3,6$ -triphenyl-1-aza-3,6-diphosphacycloheptane) ligands with high TOF for hydrogen evolution.⁶ Subsequently, a series of more efficient mononuclear nickel electrocatalysts were synthesized by the same group using $\text{P}^{\text{R}_2}\text{N}^{\text{R}_2}$ (1,5-diaza-3,7-diphosphacyclooctane with alkyl or aryl groups on the P and N atoms) ligands, which can catalyze the proton reduction to hydrogen with higher TOF and lower overpotential.⁷ These successful catalysts have suggested the importance of the nickel center and its surrounding environment which are both essential during hydrogen evolution process.

In some Ni-containing enzymes such as [NiFe]-hydrogenase and acetyl coenzyme A synthase (Fig. 1), the coordination sphere of the nickel center usually contains several cysteine residues as sulfur donors.^{3,8} To get deep insight into how the sulfur-rich environment facilitates corresponding redox

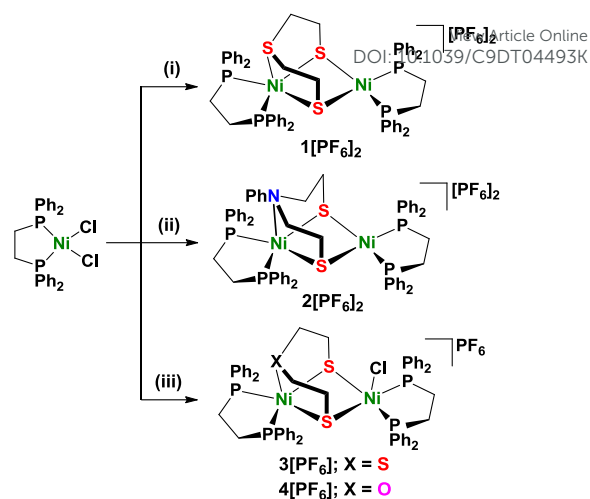
reactions, plenty of thiolate-bridged dinickel complexes were synthesized and examined toward modelling the related enzymatic activity.⁹ In contrast, there are only a few thiolate-bridged dinickel complexes constructed with respect to [NiFe]-hydrogenase mimicry.¹⁰ For example, DuBois *et al* reported several bidentate thiolate-bridged dinickel complexes supported by bidentate phosphine ligands and investigated their electrochemical properties and reactivities.^{10a} However, there is no report on the electrocatalytic hydrogen generation with this system. Recently, Bouwman and co-workers adopted thiolate-functionalized carbene ligand to construct a thiolate-bridged dinickel complex, which can realize electrocatalytic proton reduction to hydrogen.^{10c} Notably, when the ligand set contains the pyridine group as a potential proton shuttle, relatively higher catalytic activity was also observed. In this context, it is an interesting and challenging topic to construct biomimetic thiolate-bridged dinickel functional complexes featuring pendant amine with the catalytic capacity of hydrogen production.

In our preliminary work, a series of thiolate-bridged homodinuclear metallic complexes were constructed for small molecule activation and catalytic transformation.^{11–13} Recently, utilizing tridentate $S(CH_2CH_2S^-)_2$ (tpdt) or $O(CH_2CH_2S^-)_2$ (opdt), a family of homo- and heteronuclear di/multi-metallic complexes containing iron were synthesized and characterized.¹⁴ As an extension of this work, herein we adopt three different tridentate ligands containing sulfur to synthesize several novel thiolate-bridged dinickel complexes. Notably, these complexes all act as good promoters for electrocatalytic proton reduction to hydrogen, among which the dinickel complex featuring a pendant amine in the secondary coordination sphere shows the best catalytic activity.

Results and discussion

Synthesis and characterization of thiolate-bridged dinickel complexes

As illustrated in Scheme 1, four thiolate-bridged $Ni^{II}Ni^{II}$ complexes were successfully synthesized in good yields by the salt metathesis reaction. Upon treatment of mononuclear nickel precursor $[NiCl_2(dppe)]$ ($dppe = Ph_2P(CH_2)_2PPh_2$)¹⁵ with



Scheme 1 Synthesis of thiolate-bridged dinickel complexes. *Reagents and conditions:* (i) 0.5 eq. $Na_2(tpdt)$, 1 eq. NH_4PF_6 , acetone, rt, 2 h, 68%; (ii) 0.5 eq. $Li_2(npdt)$, 1 eq. NH_4PF_6 , THF, $-78^\circ C$ to rt, 73%; (iii) (a) 0.5 eq. $Na_2(tpdt)$, 0.5 eq. NH_4PF_6 , acetone, rt, 2 h, 70%; (b) 0.5 eq. $Li_2(opdt)$, 0.5 eq. NH_4PF_6 , THF, $-78^\circ C$ to rt, 70%.

0.5 equiv. of $Na_2(tpdt)$ or $Li_2(npdt)$ ($npdt = N(Ph)(CH_2CH_2S^-)_2$)¹⁶ in the presence of 1 equiv. of NH_4PF_6 , dicationic thiolate-bridged dinickel complexes $[(dppe)Ni(\mu-1,3^3SSS^-:2,2^2SS-tpdt)Ni(dppe)][PF_6]_2$ (**1**[PF_6]₂) and $[(dppe)Ni(\mu-1,3^2SS:2,2^2SS-npdt)Ni(dppe)][PF_6]_2$ (**2**[PF_6]₂) were readily obtained. In the presence of 0.5 equiv. of NH_4PF_6 , cationic thiolate-bridged dinickel chloride complexes $[(dppe)Ni(t-Cl)(\mu-1,3^3SSS^-:2,2^2SS-tpdt)Ni(dppe)][PF_6]$ (**3**[PF_6]) and $[(dppe)Ni(t-Cl)(\mu-1,3^2SSO:2,2^2SS-opdt)Ni(dppe)][PF_6]$ (**4**[PF_6]) were smoothly generated under similar conditions. Notably, complex **1**[PF_6]₂ can interact with nBu_4NCl to give **3**[PF_6] in moderate yield. Reversibly, complex **3**[PF_6] can also be readily transformed into **1**[PF_6]₂ in the presence of NH_4PF_6 . These complexes are all stable whether in the solid-state or in solution under inert gas atmosphere.

These complexes were all fully characterized by various spectroscopic methods. The 1H NMR spectroscopic results clearly indicate these complexes are all diamagnetic species consisting of two low-spin Ni^{II} ions. In the 1H NMR spectrum of **1**[PF_6]₂, two multiplets and a very broad peak at around 2.60 ppm with integral area for 12H are assigned to the four CH_2

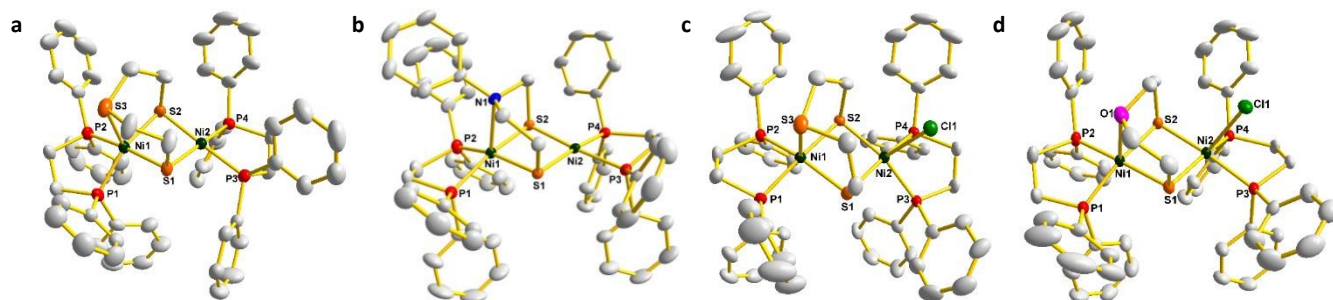


Fig. 2 Molecular structures of thiolate-bridged dinickel complexes **1**[BPh_4]₂ (a), **2**[PF_6]₂ (b), **3**[PF_6] (c) and **4**[PF_6] (d). Thermal ellipsoids are shown at 50% probability level. Hydrogen atoms and counter anions PF_6^- or BPh_4^- are omitted for clarity.

Table 1 Selected bond lengths [Å] and angles [°] of complexes **1**[BPh₄]₂, **2**[PF₆]₂, **3**[PF₆]₂ and **4**[PF₆]₂.

Complex	1 [BPh ₄] ₂	2 [PF ₆] ₂	3 [PF ₆] ₂	4 [PF ₆] ₂
Ni1...Ni2	3.1093(8)	3.2048(6)	3.2528(10)	3.2276(4)
Ni1–S1	2.238(2)	2.2574(9)	2.250(1)	2.2462(7)
Ni1–S2	2.247(2)	2.2185(9)	2.242(1)	2.2365(8)
Ni1–P1	2.183(1)	2.1757(10)	2.158(2)	2.1790(8)
Ni1–P2	2.174(2)	2.1731(10)	2.180(2)	2.1701(8)
Ni1–X ^a	2.391(2)	2.475(3)	2.392(2)	2.377(2)
Ni2–S1	2.217(2)	2.2378(9)	2.239(2)	2.2533(8)
Ni2–S2	2.237(2)	2.2283(8)	2.244(1)	2.2390(7)
Ni2–P3	2.178(2)	2.1754(9)	2.170(1)	2.1934(7)
Ni2–P4	2.168(2)	2.1872(10)	2.188(2)	2.1750(8)
Ni2–Cl1	–	–	2.614(2)	2.5955(8)
S1–Ni1–S2	87.86(6)	87.86(3)	86.55(5)	87.34(3)
S1–Ni2–S2	88.64(5)	88.11(3)	86.77(5)	87.10(3)
Ni1S1S2/Ni2S1S2	28.57(5)	9.71(3)	9.70(4)	13.18(1)
Ni1S1S2/Ni1P1P2	25.55(6)	25.55(6)	22.07(6)	15.26(2)

^aX = S, N, O

View Article Online
DOI: 10.1039/C9DT04493K

groups of the tpdt ligand and two CH₂ groups of the dppe ligands. The other two multiplets at 1.15 and 0.18 ppm at a 1:1 ratio are attributed to the other two CH₂ groups of the dppe ligands. These assignments were in good agreement with the ¹H,¹H-COSY spectroscopic results.

Differently, the ¹H NMR spectrum of **2**[PF₆]₂ shows two broad peaks with equal integral area at 2.22, 2.68 ppm for the CH₂ groups of the npdt ligand and two singlets at 1.35, 2.98 ppm with 1:1 integral ratio for the methylene groups of the two equivalent dppe ligands. Notably, the proton signals of the phenyl group in the npdt ligand appear at 6.49, 7.14 and 7.23 ppm, which is up-field shifted compared to the corresponding phenyl resonances of the dppe ligands. Distinct from the obvious overlap of signals in the ¹H NMR spectrum of **1**[PF₆]₂, complex **3**[PF₆]₂ displays six separate resonances in the region from 0.05 to 3.26 ppm, which are clearly assigned to the methylene groups of the tpdt and dppe ligands, respectively. Similar to **2**[PF₆]₂, the ¹H NMR spectrum of **4**[PF₆]₂ displays two sets of signals at a 1:1 ratio for the CH₂ groups of opdt and dppe ligands. All assignments of above ¹H NMR data are fully consistent with the ¹³C NMR spectra.

The ³¹P{¹H} NMR spectra of **1**[PF₆]₂ and **3**[PF₆]₂ both show two singlets and one septet. Using **1**[PF₆]₂ as an example, the two singlets at δ 57.8 and 63.1 ppm are attributed to phosphorus atoms of two inequivalent dppe ligands. The septet at δ –144.3 ppm is attributed to the phosphorus atoms of two PF₆ anions.¹⁷ Different from **1**[PF₆]₂ and **3**[PF₆]₂, the ³¹P{¹H} NMR spectra of **2**[PF₆]₂ and **4**[PF₆]₂ both exhibit only one singlet and one septet. These results suggest the geometric arrangements of complexes **2**[PF₆]₂ and **4**[PF₆]₂ should be symmetric in solution. For **2**[PF₆]₂, one possible explanation is that the pendant amine is dynamic in solution, which can shuttle between the two nickel centers. For complex **4**[PF₆]₂, similar phenomenon should be also observed at the pendant oxygen site. Meanwhile, the terminal chloride group of **4**[PF₆]₂ should shift to the bridging site between the two

nickel centers in the solution state. Only in this case, it is reasonable that there is only one resonance observed for two dppe ligands in the ³¹P{¹H} NMR spectrum. Furthermore, the electrospray ionization high-resolution mass spectrometry (ESI-HRMS) and elemental analysis provide further strong evidence for their molecular compositions.

X-ray crystallographic analysis of thiolated-bridged dinickel complexes

The crystal structures of these complexes were all well-defined by X-ray diffraction analysis except for **1**[PF₆]₂, whose structural information was provided by counter anion exchange product **1**[BPh₄]₂. The ORTEP of **1**[BPh₄]₂, **2**[PF₆]₂, **3**[PF₆]₂ and **4**[PF₆]₂ are shown in Fig. 2 and the selected bond distances and angles are collectively given in Table 1. The molecular structures of these complexes all contain a butterfly-shaped {Ni₂(μ-S)₂} core geometric framework. The Ni1S1S2/Ni2S1S2 dihedral angle of **1**[BPh₄]₂ is 28.57(5)°, which is obviously bigger than those of the coordinatively saturated complexes **3**[PF₆]₂ and **4**[PF₆]₂ (9.70(4) and 13.18(1)°). Notably, this dihedral angle of structurally similar complex **2**[PF₆]₂ is also small (9.71(3)°), which is due to the steric hindrance between the phenyl rings of npdt and dppe ligands. The distances between the two nickel centers in these complexes are 3.1093(8)–3.2528(10) Å, which exclude the existence of the metal–metal bond interaction. These values fall in the range of those of reported thiolate-bridged dinickel complexes supported by phosphine or Cp ligands.^{10a,10d,18} In these complexes, the five-coordinate Ni1 centres all adopt a distorted tetragonal pyramid configuration with the Ni1S1S2/Ni1P1P2 dihedral angles of 15.26(2)–25.55(6)°, and the pendant S, O or N atom of the tridentate ligands occupies the apical site. The Ni2 center of complexes **1**[BPh₄]₂ and **2**[PF₆]₂ both adopt a square-planar arrangement with Ni2S1S2/Ni2P3P4 dihedral angles of 3.65(6) and 8.45(4)°. Differently, due to the presence of the terminal chloride group,

Table 2 Electrochemical data of **1**[PF₆]₂, **2**[PF₆]₂, **3**[PF₆] and **4**[PF₆].^a

Complex	1st $E_{1/2}^{\text{red}}$ (V)		2nd $E_{1/2}^{\text{red}}$ or E_p^{red} (V)		i_{cat}/i_p^b	Overpotential (mV) ^c
	CH ₂ Cl ₂	MeCN	CH ₂ Cl ₂	MeCN		
1 [PF ₆] ₂	-1.13	-1.23	-1.56	-1.49	6.9	500
2 [PF ₆] ₂	-1.10	-0.75, -0.95	-1.40	-1.17, -1.31	11.6	420
3 [PF ₆]	-1.15	-1.24	-1.56	-1.47	4.6	510
4 [PF ₆]	-1.19	-1.25	-1.42	-1.41	8.9	490

View Article Online

DOI: 10.1039/C9DT04493K

^aDinickel complexes (1 mM) recorded at scan rate of 100 mV/s with ⁿBu₄NPF₆ (0.1 M) as supporting electrolyte. ^b i_{cat} is denoted as the catalytic current at the 10 mM TFA in MeCN. ^cOverpotentials were estimated by the standard potential for hydrogen evolution from TFA (10 mM) in MeCN. All potentials are referred to the Fc⁺⁰ redox couple.

the Ni₂ centers of complexes **3**[PF₆] and **4**[PF₆] are in a distorted tetragonal pyramid geometry with Ni₂S₁S₂/Ni₂P₃P₄ dihedral angles of 21.54(4) and 21.65(2)°. In addition, all Ni–P and Ni–S_{bridge} bond lengths in these complexes locate in the common range of reported complexes with a NiP₂S₂ subunit.¹⁹

The Ni1–S3 bond lengths of 2.391(2) and 2.392(2) Å in **1**[BPh₄]₂ and **3**[PF₆] are significantly longer than those of the Ni1–S1 and Ni1–S2 bonds. However, the Ni1–S3 bond lengths in these two complexes still fall in the range of common Ni–S bond length.²⁰ It suggests the existence of the strong bonding interaction between the nickel center and the thioether sulfur atom, which means it is difficult that the Ni1–S3 bond spontaneously breaks in the solution state. This proposal is fully consistent with the experimental fact that there are two inequivalent resonances with similar intensity for dppe ligands in the ³¹P{¹H} NMR spectra of **1**[PF₆]₂ and **3**[PF₆].

In complex **2**[PF₆]₂, the Ni–N distance is 2.475(3) Å, which is obviously longer than common Ni–N bond lengths in some nickel complexes²¹ and other metal-nitrogen bond lengths in mononuclear metal complexes possessing pendant nitrogen group.²² However, this bond distance is remarkably shorter than the sum of the van der Waal's radii (3.18 Å). Therefore, there should be a weak bond interaction between the nickel center and the pendant nitrogen atom in **2**[PF₆]₂. The elongation of the Ni–N distance is likely caused by steric hindrance between the dppe ligand and the phenyl of the pendant amine group. This weak coordination mode in this system provides the possibility of the dynamic transformation in solution as above mentioned. Similar situation should be also observed in **4**[PF₆], because the Ni–O distance of 2.377(2) Å is beyond the common range of the Ni–O bond length in previously reported nickel complexes.²³

Electrochemical studies of thiolated-bridged dinickel complexes

Firstly, the redox properties of four thiolate-bridged dinickel complexes in MeCN and CH₂Cl₂ were explored by cyclic voltammetry and their electrochemical data were summarized in Table 2 (see ESI for CV traces). In the cyclic voltammograms of **1**[PF₆]₂, **3**[PF₆] and **4**[PF₆] in CH₂Cl₂, the first reduction event is quasi-reversible and the second one

is irreversible. Differently, the two reduction waves of complex **2**[PF₆]₂ at $E_p^{\text{red}} = -1.10$ and -1.40 V versus Fc⁺⁰ are both irreversible. These complexes all undergo two successive one-electron reduction processes assigned to the Ni^{II}Ni^{II}/Ni^INi^I and Ni^{II}Ni^I/Ni^INi^I couples,^{10a} which are in good agreement with the experimental fact that the reduction peak currents of the two redox couples are close to that of equivalent ferrocene (Fc) as an internal standard. Notably, reduction potentials of complex **2**[PF₆]₂ featuring pendant amine are shifted positively compared with other three complexes. Interestingly, when the solvent was changed from CH₂Cl₂ to MeCN, there are three quasi-reversible and an irreversible reduction processes observed (Figure S35). These significant changes of the reduction events in different solvents may be due to the formation of a new species with coordinated MeCN. However, when we revisited the ¹H NMR spectrum of complex **2**[PF₆]₂ in CD₃CN, no expected new species was detected compared with its ¹H NMR spectrum in CD₂Cl₂. Based on above results, we considered MeCN can reversibly bind to the nickel center under electrochemical conditions, which generates an equilibrium mixture of **2**[PF₆]₂ and potential complex **2**(MeCN)[PF₆]₂. That is why the CV curve of **2**[PF₆]₂ in CD₃CN appears four reduction waves. The first and third

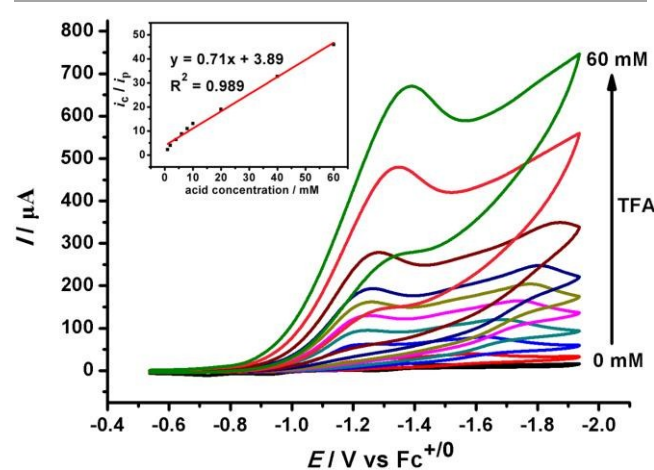


Fig. 3 Cyclic voltammograms of **2**[PF₆]₂ (1 mM in 0.1 M ⁿBu₄NPF₆ in MeCN under Ar) with increments of TFA (0, 1, 2, 4, 8, 10, 20, 40 and 60 mM). Inset: i_{cat}/i_p dependence with increasing acid concentration at 100 mV s⁻¹.

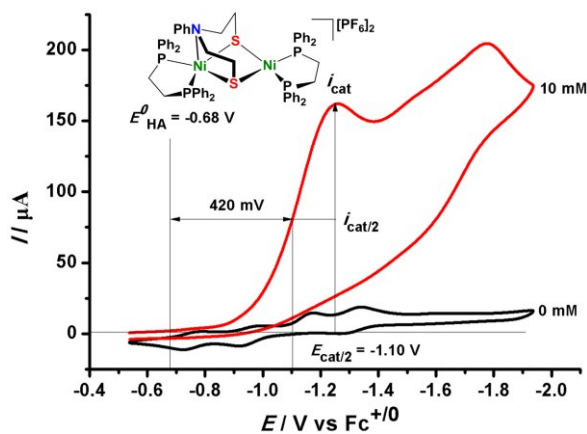


Fig. 4 Determination of the overpotential of **2[PF₆]₂** (1 mM) in the presence of 10 mM TFA in MeCN.

reduction waves are assigned to complex **2[PF₆]₂**, and the other two reduction processes belong to the proposed species **2(MeCN)[PF₆]₂**. Furthermore, a plot of the peak current of reduction wave (i_p) vs square root of scan rate shows a linear correlation, implying diffusion-controlled electrochemical reduction events.²⁴

One step further, the electrocatalytic activity of these complexes for proton reduction was explored by cyclic voltammetry. As shown in Fig. 3, complex **2[PF₆]₂** was chosen as a representative electrocatalyst for the reduction of trifluoroacetic acid (TFA, $pK_a^{\text{MeCN}} = 12.65$).²⁵ Upon addition of 2 equiv. of TFA, a broad reductive peak appeared at -1.19 V. As the acid concentration increased, peak current of this reduction event increased linearly and the potential is shifted toward more negative cathodic values. These observations are all diagnostic to the electrocatalysis of proton reduction. Furthermore, we carried out the bulk electrolysis of 1 mM **2[PF₆]₂** in the presence of 60 mM TFA at -1.20 V. After electrolysis over a 0.5 h period, about $1.60 \mu\text{mol}$ of H_2 was detected by gas chromatography and 0.32 C charges had passed through the cell corresponding to the theoretical H_2 production of $1.68 \mu\text{mol}$. Hence, the Faraday efficiency for H_2 was calculated to be 95%. In addition, the control experiment that acid reduction in the absence of catalyst was also conducted, however, no catalytic peak was observed at corresponding potential. Moreover, the rinse test was performed in which the working electrode was rinsed several times with MeCN following the catalytic cyclic voltammetry and then transferred to a fresh solution of TFA in MeCN. No observation of catalytic peak suggests the active species is molecule in solution not nickel deposit on the electrode.

To further assess the catalytic activity, we next explored some important evaluating parameters.²⁶ Current enhancement of the reductive peak is an essential indicator for comparison of catalytic capacity of metal complexes.²⁷ Hence, we first calculated the i_c/i_p ratio value in the presence of 10 mM TFA, which means the ratio of catalytic current (i_c) to reductive peak current (i_p). As listed in Table 2, complex **2[PF₆]₂** shows the best catalytic activity, whose i_c/i_p ratio value is up to 11.6. In addition,

the overpotential is the other important metrics for evaluating the catalytic activity of hydrogen evolution. Due to the homoconjugation effect, TFA exhibits a significantly low pK_a value in MeCN, which obviously impacts the half-wave potential of TFA reduction. Based on this understanding, we calculated the overpotentials of these thiolate-bridged dinickel complexes by the updated method reported by Helm and Appel.²⁸ At 10 mM TFA in MeCN, $E_{\text{TFA}^+} = -0.68$ V versus $\text{Fc}^{+/0}$,²⁹ and the overpotential for **2[PF₆]₂** was calculated to be 0.42 V using $E_{\text{cat}/2} = -1.10$ V versus $\text{Fc}^{+/0}$ (Fig. 4). The overpotential of **2[PF₆]₂** is slightly lower than those of complexes **1[PF₆]₂**, **3[PF₆]₂** and **4[PF₆]₂**. Although inferior to some mononuclear nickel complexes supported by phosphine ligands,³⁰ complex **2[PF₆]₂** is obviously superior to other previously reported thiolate-bridged dinuclear complexes,^{10b,10c,10e,23c,27c,31} Superior catalytic performance of **2[PF₆]₂** suggests that the pendant amine group may behave as a proton relay similar to some reported functional complexes for hydrogen formation.³²

Conclusions

In summary, a series of biomimetic thiolate-bridged dinickel complexes were designed and synthesized, which were all proven as promoters for electrocatalytic hydrogen production. Remarkably, the incorporation of a pendant amine into the bridging dithiolate ligand as proton relay facilitates enhancement of the catalytic activity at relatively low overpotential in this dinickel system. It bodes well for future work on catalytic transformations of other small molecules such as N_2 , which may involve complicated multi-proton, multi-electron reduction processes.

Experimental

General Procedures.

All manipulations were routinely conducted under inert gas atmosphere in a glovebox or by standard Schlenk techniques. All solvents were dried and distilled over an appropriate drying agent under argon. Precursor complex $[\text{NiCl}_2(\text{dppe})]$ ¹⁵ and ligand $\text{N}(\text{Ph})(\text{CH}_2\text{CH}_2\text{SH})_2$ ¹⁶ were prepared according to literature procedures. NH_4PF_6 (Aldrich), NaBPh_4 (Aldrich), $\text{S}(\text{CH}_2\text{CH}_2\text{SH})_2$ (Aldrich), $\text{O}(\text{CH}_2\text{CH}_2\text{SH})_2$ (Aldrich), CF_3COOH (Aldrich), $^n\text{BuLi}$ (Aldrich), NaH (Aldrich), $^n\text{Bu}_4\text{NCl}$ (Aldrich) and $^n\text{Bu}_4\text{NPF}_6$ (Aldrich) were used without further purification.

Spectroscopic Measurements.

The ^1H , $^{13}\text{C}\{^1\text{H}\}$ and $^{31}\text{P}\{^1\text{H}\}$ NMR spectra were recorded on a Bruker 400 Ultra Shield spectrometer. The ^1H , ^1H -COSY spectrum was recorded on a Bruker 500 Ultra Shield spectrometer. The chemical shifts (δ) are given in parts per million relative to CD_2Cl_2 (5.32 ppm for ^1H , 53.84 ppm for ^{13}C). Infrared spectra were recorded on a NEXVSTM FT-IR spectrometer. ESI-HRMS were recorded on a HPLC/Q-ToF micro spectrometer. Elemental analyses were performed on a Vario EL analyzer.

X-ray Crystallography Procedures.

The data were obtained on a Bruker SMART APEX CCD diffractometer with graphite-monochromated Mo K α radiation ($\lambda = 0.71073 \text{ \AA}$). Empirical absorption corrections were performed using the SADABS program.³³ Structures were solved by direct methods and refined by full-matrix least-squares based on all data using SHELX97.³⁴ All of the non-hydrogen atoms were refined anisotropically. All of the hydrogen atoms were generated and refined in ideal positions and refined with fixed isotropic displacement parameters.

Electrochemistry.

Electrochemical measurements were recorded using a BAS-100W electrochemical potentiostat at a scan rate of 100 mV/s. Electrochemical experiments were carried out in a three-electrode cell under argon at room temperature. The working electrode was a glassy carbon disk (diameter 3 mm), the reference electrode was a nonaqueous Ag/Ag⁺ electrode, the auxiliary electrode was a platinum wire, and the supporting electrolyte was 0.1 M ⁿBu₄NPF₆ in MeCN. Electrocatalysis studies were performed by the stepwise addition of different amounts of CF₃COOH (TFA) with microsyringe. Controlled potential electrolysis experiments were carried out in a two-compartment, gas-tight, H-type electrolysis cell under argon at room temperature. The working electrode was a glassy carbon disk (diameter 3 mm), the reference electrode was a nonaqueous Ag/Ag⁺ electrode, and the auxiliary electrode was a platinum sheet. All potentials reported herein are quoted relative to the FeCp₂/FeCp₂⁺ couple. Gas analysis was performed with a Techcomp GC7900 gas chromatography instrument with argon as the carrier gas and a thermal conductivity detector.

Preparation of [(dppe)Ni(μ -1, κ ³SSS':2, κ ²SS-tpdt)Ni(dppe)][PF₆]₂ (1[PF₆]₂)

Method A: At room temperature, a suspension of Na₂(tpdt) (tpdt = S(CH₂CH₂S⁻)₂) in acetone (10 mL), prepared by the reaction of NaH (12 mg, 0.50 mmol) and S(CH₂CH₂SH)₂ (39 mg, 0.25 mmol), was transferred via a cannula to a solution of [NiCl₂(dppe)] (264 mg, 0.50 mmol) in acetone (15 mL) and then NH₄PF₆ (82 mg, 0.50 mmol) was added to the reaction solution. The mixture was vigorously stirred for 2 h. After all volatiles were removed under vacuum, the residues were extracted with CH₂Cl₂ (3 \times 10 mL) and then dried *in vacuo*. Finally, the residues were washed with THF (3 \times 10 mL). The product [(dppe)Ni(μ -1, κ ³SSS':2, κ ²SS-tpdt)Ni(dppe)][PF₆]₂ (1[PF₆]₂, 231 mg, 0.17 mmol, 68%), was obtained as a brownish-yellow powder. ¹H NMR (400 MHz, CD₂Cl₂, ppm): δ 0.18-2.65 (m, 8H, Ph₂P(CH₂)₂PPh₂), 2.51-2.63 (m, 8H, tpdt-H), 7.36-8.01 (m, 40H, Ph-H). ¹³C{¹H} NMR (100 MHz, CD₂Cl₂, ppm): δ 27.0 (PCH₂), 30.0 (PCH₂), 34.8 (SCH₂), 36.5 (SCH₂), 129.7 (Ph-C), 130.3 (Ph-C), 133.1 (Ph-C), 133.4 (Ph-C), 133.6 (Ph-C), 133.9 (Ph-C). ³¹P{¹H} NMR (162 MHz, CD₂Cl₂, ppm): δ -144.3 (septet, PF₆⁻), 57.8 (s), 63.1 (s). IR (film; cm⁻¹): 3060, 2927, 1437, 1109, 841, 695, 517. ESI-HRMS: Calcd. For [1]²⁺ 532.0601; Found 532.0626. Anal. Calcd. For C₅₆H₅₆F₁₂Ni₂P₆S₃·THF: C, 50.45; H, 4.52. Found: C, 50.61; H, 4.62.

Method B: At room temperature, to a brownish-yellow solution

of 3[PF₆] (125 mg, 0.10 mmol) in MeCN (10 mL) was added NH₄PF₆ (16 mg, 0.10 mmol) with vigorous stirring for 1 h. The solution was evaporated to dryness under reduced pressure. The residue was washed with *n*-hexane for three times, extracted with CH₂Cl₂ (20 mL) and then dried *in vacuo*. The product, [(dppe)Ni(μ -1, κ ³SSS':2, κ ²SS-tpdt)Ni(dppe)][PF₆]₂ (1[PF₆]₂, 111 mg, 0.08 mmol, 80%), was obtained as a brownish-yellow powder.

Using the similar synthetic method except for the replacement of NH₄PF₆ by NaBPh₄, 1[BPh₄]₂ was smoothly obtained in 65% yield. Crystals suitable for X-ray diffraction were obtained from a saturated CH₂Cl₂ solution layered with *n*-hexane at room temperature. ¹H NMR (400 MHz, CD₂Cl₂, ppm): δ 0.01-2.05 (m, 8H, Ph₂P(CH₂)₂PPh₂), 2.15-2.68 (m, 8H, tpdt-H), 6.82-7.24 (m, 40H, BPh₄-H), 7.32-7.93 (m, 40H, Ph-H). ¹³C{¹H} NMR (100 MHz, CD₂Cl₂, ppm): δ 26.3 (PCH₂), 29.9 (PCH₂), 34.6 (SCH₂), 36.6 (SCH₂), 122.2 (BPh₄-C), 126.0 (BPh₄-C), 129.8 (Ph-C), 130.4 (Ph-C), 132.8 (Ph-C), 133.6 (Ph-C), 134.0 (Ph-C), 136.3 (BPh₄-C). ³¹P{¹H} NMR (162 MHz, CD₂Cl₂, ppm): δ 58.5(s), 63.4(s). IR (film; cm⁻¹): 3059, 1432, 1101, 702, 524. ESI-HRMS: Calcd. For [1]²⁺ 532.0601; Found 532.0604. Anal. Calcd. For C₁₀₄H₉₆B₂Ni₂P₄S₃: C, 73.26; H, 5.68. Found: C, 73.59; H, 5.76.

Preparation of [(dppe)Ni(μ -1, κ ²SS:2, κ ²SS-npdt)Ni(dppe)][PF₆]₂ (2[PF₆]₂)

At -78 °C, a suspension of Li₂(npdt) (npdt = N(Ph)(CH₂CH₂S⁻)₂) in THF (10 mL), prepared by the reaction of ⁿBuLi (0.36 mL, 2.2 M solution in *n*-hexane, 0.80 mmol) and N(Ph)(CH₂CH₂SH)₂ (85 mg, 0.40 mmol) at 0 °C, was transferred via a cannula to a cooled solution of [NiCl₂(dppe)] (422 mg, 0.80 mmol) in THF (15 mL) and then NH₄PF₆ (130 mg, 0.80 mmol) was added to the reaction solution. The mixture was vigorously stirred at -78 °C to room temperature. After all volatiles were removed under vacuum, the residues were extracted with CH₂Cl₂ (3 \times 10 mL) and then dried *in vacuo*. Finally, the residues were washed with THF (3 \times 10 mL). The product, [(dppe)Ni(μ -1, κ ²SS:2, κ ²SS-npdt)Ni(dppe)][PF₆]₂ (2[PF₆]₂, 408 mg, 0.29 mmol, 73%), was obtained as a brownish-red powder. Crystals suitable for X-ray diffraction were obtained from a saturated CH₂Cl₂ solution layered with *n*-hexane at room temperature. ¹H NMR (400 MHz, CD₂Cl₂, ppm): δ 1.35 (br, 4H, Ph₂P(CH₂)₂PPh₂), 2.22-2.68 (br, 8H, npdt-CH₂), 2.98 (br, 4H, Ph₂P(CH₂)₂PPh₂), 6.49-7.23 (m, 5H, NPh-H), 7.32-8.09 (m, 40H, PPh-H). ¹³C{¹H} NMR (100 MHz, CD₂Cl₂, ppm): δ 27.0 (PCH₂), 31.0 (SCH₂), 32.7 (NCH₂), 119.3 (NPh-C), 123.8 (NPh-C), 130.0 (PPh-C), 130.1 (PPh-C), 132.4 (PPh-C), 132.8 (PPh-C), 133.4 (PPh-C), 134.1 (PPh-C), 151.5 (NPh-C). ³¹P{¹H} NMR (162 MHz, CD₂Cl₂, ppm): δ -144.3 (septet, PF₆⁻), 54.4 (s). IR (film; cm⁻¹): 1438, 1101, 840, 693, 526. ESI-HRMS: Calcd. For [2]²⁺ 561.5952; Found 561.5931. Anal. Calcd. For C₆₂H₆₁F₁₂NNi₂P₆S₂: C, 52.61; H, 4.34; N, 0.99. Found: C, 52.69; H, 4.79; N, 1.29.

Preparation of [(dppe)Ni(*t*-Cl)(μ -1, κ ³SSS':2, κ ²SS-tpdt)Ni(dppe)][PF₆]₃ (3[PF₆])

Method A: At room temperature, a suspension of Na₂(tpdt) in acetone (10 mL), prepared by the reaction of NaH (10 mg, 0.40 mmol) and S(CH₂CH₂SH)₂ (31 mg, 0.20 mmol), was transferred via a cannula to a solution of [NiCl₂(dppe)] (211 mg, 0.40 mmol)

in acetone (10 mL) and then NH_4PF_6 (33 mg, 0.20 mmol) was added to the reaction solution. The mixture was vigorously stirred for 2 h. After all volatiles were removed under vacuum, the residues were extracted with CH_2Cl_2 (3×10 mL) and then dried *in vacuo*. The product, $[(\text{dppe})\text{Ni}(\text{t-Cl})(\mu\text{-}1\text{-}\kappa^3\text{SSS}':2\text{-}\kappa^2\text{SS-tpdt})\text{Ni}(\text{dppe})][\text{PF}_6]$ (**3**)[PF_6], 175 mg, 0.14 mmol, 70%), was obtained as a brownish-yellow powder. Crystals suitable for X-ray diffraction were obtained from a saturated MeCN solution layered with Et_2O at room temperature. ^1H NMR (400 MHz, CD_2Cl_2 , ppm): δ 0.05-3.26 (m, 8H, $\text{Ph}_2\text{P}(\text{CH}_2)_2\text{PPh}_2$), 2.21-2.79 (br, 8H, *tpdt-H*), 7.25-8.33 (m, 40H, *Ph-H*). $^{13}\text{C}\{^1\text{H}\}$ NMR (100 MHz, CD_2Cl_2 , ppm): δ 27.9 (PCH_2), 29.5 (PCH_2), 34.5 (SCH_2), 35.6 (SCH_2), 127.9 (*Ph-C*), 129.3 (*Ph-C*), 129.6 (*Ph-C*), 130.8 (*Ph-C*), 131.5 (*Ph-C*), 133.7 (*Ph-C*), 134.2 (*Ph-C*), 134.5 (*Ph-C*). $^{31}\text{P}\{^1\text{H}\}$ NMR (162 MHz, CD_2Cl_2 , ppm): δ -144.4 (septet, PF_6^-), 54.4 (s), 57.6 (s). IR (film; cm^{-1}): 3059, 2920, 1438, 1109, 840, 694, 525. ESI-HRMS: Calcd. For **3** $^+$ 1099.0890; Found 1099.0873. Anal. Calcd. For $\text{C}_{56}\text{H}_{56}\text{ClF}_6\text{Ni}_2\text{P}_5\text{S}_3\cdot\text{Et}_2\text{O}$: C, 54.55; H, 5.04. Found: C, 54.61; H, 4.84.

Method B: At room temperature, to a brownish-yellow solution of **1**[PF_6] $_2$ (136 mg, 0.10 mmol) in MeCN (10 mL) was added $n\text{Bu}_4\text{NCl}$ (28 mg, 0.10 mmol) with vigorous stirring for 3 h. The solution was evaporated to dryness under reduced pressure. The residue was washed with *n*-hexane for three times, extracted with THF (20 mL) and then dried *in vacuo*. The product, $[(\text{dppe})\text{Ni}(\text{t-Cl})(\mu\text{-}1\text{-}\kappa^3\text{SSS}':2\text{-}\kappa^2\text{SS-tpdt})\text{Ni}(\text{dppe})][\text{PF}_6]$ (**3**)[PF_6] $_2$, 50 mg, 0.04 mmol, 40%), was obtained as a brownish-yellow powder.

Preparation of $[(\text{dppe})\text{Ni}(\text{t-Cl})(\mu\text{-}1\text{-}\kappa^3\text{SSO}:2\text{-}\kappa^2\text{SS-opdt})\text{Ni}(\text{dppe})][\text{PF}_6]$ (**4**)[PF_6]

At -78°C , a suspension of $\text{Li}_2(\text{opdt})$ ($\text{opdt} = \text{O}(\text{CH}_2\text{CH}_2\text{S}^-)_2$) in THF (10 mL), prepared by the reaction of $n\text{BuLi}$ (0.45 mL, 2.2 M solution in *n*-hexane, 1.0 mmol) and $\text{O}(\text{CH}_2\text{CH}_2\text{SH})_2$ (69 mg, 0.50 mmol) at 0°C , was transferred via a cannula to a cooled solution of $[\text{NiCl}_2(\text{dppe})]$ (528 mg, 1.0 mmol) in THF (15 mL) and then NH_4PF_6 (82 mg, 0.50 mmol) was added to the reaction solution. The mixture was vigorously stirred at -78°C to room temperature. After all volatiles were removed under vacuum, the residues were extracted with CH_2Cl_2 (3×10 mL) and then dried *in vacuo*. The product, $[(\text{dppe})\text{Ni}(\text{t-Cl})(\mu\text{-}1\text{-}\kappa^3\text{SSO}:2\text{-}\kappa^2\text{SS-opdt})\text{Ni}(\text{dppe})][\text{PF}_6]$ (**4**)[PF_6], 437 mg, 0.35 mmol, 70%), was obtained as a brownish-red powder. Crystals suitable for X-ray diffraction were obtained from a saturated CH_2Cl_2 solution layered with *n*-hexane at room temperature. ^1H NMR (400 MHz, CD_2Cl_2 , ppm): δ 1.45-2.18 (br, 8H, *opdt-CH}_2), 2.72-3.57 (br, 8H, $\text{Ph}_2\text{P}(\text{CH}_2)_2\text{PPh}_2$), 7.35-7.95 (m, 40H, *Ph-H*). $^{13}\text{C}\{^1\text{H}\}$ NMR (100 MHz, CD_2Cl_2 , ppm): δ 27.4 (PCH_2), 28.1 (PCH_2), 31.8 (SCH_2), 67.2 (OCH_2), 128.8 (*Ph-C*), 129.3 (*Ph-C*), 131.5 (*Ph-C*), 132.1 (*Ph-C*), 133.3 (*Ph-C*), 134.0 (*Ph-C*). $^{31}\text{P}\{^1\text{H}\}$ NMR (162 MHz, CD_2Cl_2 , ppm): δ -144.4 (septet, PF_6^-), 53.8 (s). IR (film; cm^{-1}): 3059, 2921, 1431, 1101, 840, 695, 524. ESI-HRMS: Calcd. For **4** $^+$ 1083.1118; Found 1083.1136. Anal. Calcd. For $\text{C}_{56}\text{H}_{56}\text{ClF}_6\text{Ni}_2\text{OP}_5\text{S}_2$: C, 54.64; H, 4.59. Found: C, 54.75; H, 4.42.*

Acknowledgements

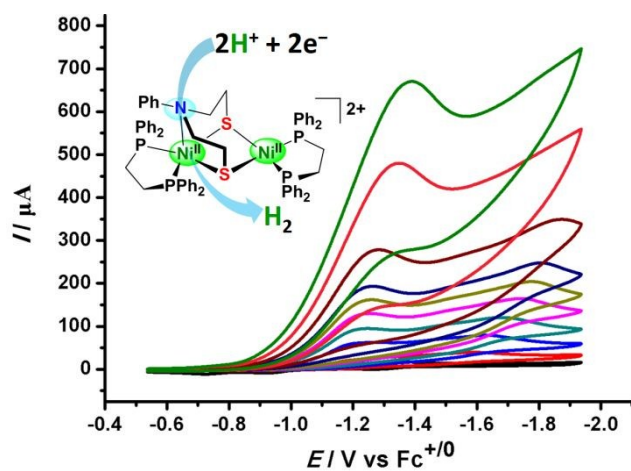
This work was supported by the National Natural Science Foundation of China (Nos. 21690064, 101571026), the Program for Changjiang Scholars and Innovative Research Team in University (No. IRT13008), the "111" project of the Ministry of Education of China and the Fundamental Research Funds for the Central Universities (DUT19RC(3)013).

Notes and references

- 1 T. R. Cook, D. K. Dogutan, S. Y. Reece, Y. Surendranath, T. S. Teets and D. G. Nocera, *Chem. Rev.*, 2010, **110**, 6474-6502.
- 2 (a) V. Artero and M. Fontecave, *Coord. Chem. Rev.*, 2005, **249**, 1518-1535; (b) J.-F. Capon, F. Gloaguen, P. Schöllhammer and J. Talarmin, *Coord. Chem. Rev.*, 2005, **249**, 1664-1676; (c) S. Fukuzumi, Y. Yamada, T. Suenobu, K. Ohkubo and H. Kotani, *Energy Environ. Sci.*, 2011, **4**, 2754-2766; (d) M. Wang, L. Chen and L. Sun, *Energy Environ. Sci.*, 2012, **5**, 6763-6778; (e) D. L. DuBois, *Inorg. Chem.*, 2014, **53**, 3935-3960.
- 3 (a) J. C. Fontecilla-Camps, A. Volbeda, C. Cavazza and Y. Nicolet, *Chem. Rev.*, 2007, **107**, 4273-4303; (b) W. Lubitz, H. Ogata, O. Rüdiger and E. Reijerse, *Chem. Rev.*, 2014, **114**, 4081-4148.
- 4 (a) C. Tard and C. J. Pickett, *Chem. Rev.*, 2009, **109**, 2245-2274; (b) T. R. Simmons, G. Berggren, M. Bacchi, M. Fontecave and V. Artero, *Coord. Chem. Rev.*, 2014, **270-271**, 127-150; (c) D. Schilter, J. M. Camara, M. T. Huynh, S. Hammes-Schiffer and T. B. Rauchfuss, *Chem. Rev.*, 2016, **116**, 8693-8749.
- 5 (a) S. Canaguier, V. Artero and M. Fontecave, *Dalton Trans.*, 2008, 315-325; (b) R. M. Bullock, A. M. Appel and M. L. Helm, *Chem. Commun.*, 2014, **50**, 3125-3143.
- 6 M. L. Helm, M. P. Stewart, R. M. Bullock, M. Rakowski DuBois and D. L. DuBois, *Science*, 2011, **333**, 863-866.
- 7 (a) A. J. Cardenas, B. Ginovska, N. Kumar, J. Hou, S. Raugel, M. L. Helm, A. M. Appel, R. M. Bullock and M. O'Hagan, *Angew. Chem. Int. Ed.*, 2016, **55**, 13509-13513; (b) C. M. Klug, A. J. P. Cardenas, R. M. Bullock, M. O'Hagan and E. S. Wiedner, *ACS Catal.*, 2018, **8**, 3286-3296.
- 8 M. Can, F. A. Armstrong and S. W. Ragsdale, *Chem. Rev.*, 2014, **114**, 4149-4174.
- 9 (a) E. Bouwman and J. Reedijk, *Coord. Chem. Rev.*, 2005, **249**, 1555-1581; (b) D. J. Evans, *Coord. Chem. Rev.*, 2005, **249**, 1582-1595; (c) T. C. Harrop and P. K. Mascharak, *Coord. Chem. Rev.*, 2005, **249**, 3007-3024.
- 10 (a) K. Redin, A. D. Wilson, R. Newell, M. Rakowski DuBois and D. L. DuBois, *Inorg. Chem.*, 2007, **46**, 1268-1276; (b) A. Mondragon, M. Flores-Alamo, P. R. Martínez-Alanis, G. Aullon, V. M. Ugalde-Saldívar and I. Castillo, *Inorg. Chem.*, 2015, **54**, 619-627; (c) S. Luo, M. A. Siegler and E. Bouwman, *Organometallics*, 2018, **37**, 740-747; (d) Y. X. C. Goh, H. M. Tang, W. L. J. Loke and W. Y. Fan, *Inorg. Chem.*, 2019, **58**, 12178-12183; (e) A. Mondragón-Díaz, E. Robles-Marín, B. A. Murueta-Cruz, J. C. Aquite, P. R. Martínez-Alanis, M. Flores-Alamo, G. Aullón, L. N. Benítez and I. Castillo, *Chem. Asian J.*, 2019, **14**, 3301-3312.
- 11 (a) Y. Chen, Y. Zhou, P. Chen, Y. Tao, Y. Li and J. Qu, *J. Am. Chem. Soc.*, 2008, **130**, 15250-15251; (b) Y. Chen, L. Liu, Y. Peng, P. Chen, Y. Luo and J. Qu, *J. Am. Chem. Soc.*, 2011, **133**, 1147-1149; (c) Y. Li, Y. Li, B. Wang, Y. Luo, D. Yang, P. Tong, J. Zhao, L. Luo, Y. Zhou, S. Chen, F. Cheng and J. Qu, *Nat. Chem.*, 2013, **5**, 320-326; (d) Y. Zhang, T. Mei, D. Yang, Y. Zhang, B. Wang and J. Qu, *Dalton Trans.*, 2017,

- 46, 15888-15896; (e) L. Su, D. Yang, Y. Zhang, B. Wang and J. Qu, *Chem. Commun.*, 2018, **54**, 13119-13122.
- 12 Y. Zhang, P. Tong, D. Yang, J. Li, B. Wang and J. Qu, *Chem. Commun.*, 2017, **53**, 9854-9857.
- 13 (a) X. Ji, D. Yang, P. Tong, J. Li, B. Wang and J. Qu, *Organometallics*, 2017, **36**, 1515-1521; (b) X. Zhao, D. Yang, Y. Zhang, B. Wang and J. Qu, *Chem. Commun.*, 2018, **54**, 11112-11115; (c) X. Zhao, D. Yang, Y. Zhang, B. Wang and J. Qu, *Org. Lett.*, 2018, **20**, 5357-5361.
- 14 (a) Y. Li, Y. Zhang, D. Yang, Y. Li, P. Sun, B. Wang and J. Qu, *Organometallics*, 2015, **34**, 1661-1667; (b) Y. Zhang, D. Yang, Y. Li, B. Wang, X. Zhao and J. Qu, *Dalton Trans.*, 2017, **46**, 7030-7038.
- 15 E. A. Standley, S. J. Smith, P. Müller and T. F. Jamison, *Organometallics*, 2014, **33**, 2012-2018.
- 16 S. J. Lee, J. H. Jung, J. Seo, I. Yoon, K. Park, L. F. Lindoy and S. S. Lee, *Org. Lett.*, 2006, **8**, 1641-1643.
- 17 M. Schmidtendorf, T. Pape and F. E. Hahn, *Dalton Trans.*, 2013, **42**, 16128-16141.
- 18 (a) N.-F. Ho and T. C. W. Mak, *J. Chem. Soc. Dalton Trans.*, 1990, 3591-3595; (b) D. A. Vicic and W. D. Jones, *J. Am. Chem. Soc.*, 1999, **121**, 7606-7617; (c) G. M. Chambers, T. B. Rauchfuss, F. Arrigoni and G. Zampella, *Organometallics*, 2016, **35**, 836-846.
- 19 (a) Q. Wang, A. J. Blake, E. S. Davies, E. J. L. McInnes, C. Wilson and M. Schröder, *Chem. Commun.*, 2003, 3012-3013; (b) T. C. Harrop, M. M. Olmstead and P. K. Mascharak, *J. Am. Chem. Soc.*, 2004, **126**, 14714-14715; (c) R. Krishnan and C. G. Riordan, *J. Am. Chem. Soc.*, 2004, **126**, 4484-4485.
- 20 (a) W.-F. Liaw, C.-Y. Chiang, G.-H. Lee, S.-M. Peng, C.-H. Lai and M. Y. Darensbourg, *Inorg. Chem.*, 2000, **39**, 480-484; (b) A. Perra, Q. Wang, A. J. Blake, E. S. Davies, J. McMaster, C. Wilson and M. Schröder, *Dalton Trans.*, 2009, 925-931; (c) S. Tanino, Z. Li, Y. Ohki and K. Tatsumi, *Inorg. Chem.*, 2009, **48**, 2358-2360.
- 21 (a) R. M. Jenkins, M. L. Singleton, E. Almaraz, J. H. Reibenspies and M. Y. Darensbourg, *Inorg. Chem.*, 2009, **48**, 7280-7293; (b) M. Ito, M. Kotera, T. Matsumoto and K. Tatsumi, *Proc. Natl. Acad. Sci.*, 2009, **106**, 11862-11866; (c) S. Ogo, K. Ichikawa, T. Kishima, T. Matsumoto, H. Nakai, K. Kusaka and T. Ohhara, *Science*, 2013, **339**, 682-684; (d) J. A. Denny and M. Y. Darensbourg, *Chem. Rev.*, 2015, **115**, 5248-5273.
- 22 (a) R. Y. C. Shin, G. K. Tan, L. L. Koh and L. Y. Goh, *Organometallics*, 2004, **23**, 6293-6298; (b) E. B. Hulley, M. L. Helm and R. M. Bullock, *Chem. Sci.*, 2014, **5**, 4729-4741; (c) S. Zhang and R. M. Bullock, *Inorg. Chem.*, 2015, **54**, 6397-6409; (d) Y. Zhang, T. Mei, D. Yang, Y. Zhang, B. Wang and J. Qu, *Inorg. Chem. Commun.*, 2017, **86**, 133-136.
- 23 (a) A. Famengo, D. Pinero, O. Jeannin, T. Guizouarn and M. Fourmigué, *Dalton Trans.*, 2012, **41**, 1441-1443; (b) J. A. Denny, W. S. Foley, A. D. Todd and M. Y. Darensbourg, *Chem. Sci.*, 2015, **6**, 7079-7088; (c) P. Sun, D. Yang, Y. Li, Y. Zhang, L. Su, B. Wang and J. Qu, *Organometallics*, 2016, **35**, 751-757.
- 24 A. J. Bard and L. R. Faulkner, *Electrochemical Methods: Fundamentals and Applications*; 2nd ed. Wiley: New York, 2000.
- 25 K. Izutsu, *Acid-Base Dissociation Constants in Dipolar Aprotic Solvents*; Blackwell Scientific Publications: Oxford, U.K., 1990.
- 26 K. J. Lee, N. Elgrishi, B. Kandemir and J. L. Dempsey, *Nat. Rev. Chem.*, 2017, **1**, 1-14.
- 27 (a) G. A. N. Felton, C. A. Mebi, B. J. Petro, A. K. Vannucci, D. H. Evans, R. S. Glass and D. L. Lichtenberger, *J. Organomet. Chem.*, 2009, **694**, 2681-2699; (b) S. Roy, T.-A. D. Nguyen, L. Gan and A. K. Jones, *Dalton Trans.*, 2015, **44**, 14865-14876; (c) T. Shimamura, Y. Maeno, K. Kubo, S. Kume, C. Greco and T. Mizuta, *Dalton Trans.*, 2019, **48**, 16595-16603.
- 28 A. M. Appel and M. L. Helm, *ACS Catal.*, 2014, **4**, 630-633.
- 29 (a) V. Fourmond, P. A. Jacques, M. Fontecave and V. Artero, *Inorg. Chem.*, 2010, **49**, 10338-10347; (b) M. D. Sampson and C. P. Kubiak, *Inorg. Chem.*, 2015, **54**, 6674-6676.
- 30 (a) L. Gan, T. L. Groy, P. Tarakeshwar, S. K. S. Mazinani, J. Shearer, V. Mujica and A. K. Jones, *J. Am. Chem. Soc.*, 2015, **137**, 1109-1115; (b) R. Tatematsu, T. Inomata, T. Ozawa and H. Masuda, *Angew. Chem. Int. Ed.*, 2016, **55**, 5247-5250.
- 31 (a) B. E. Barton and T. B. Rauchfuss, *J. Am. Chem. Soc.*, 2010, **132**, 14877-14885; (b) H.-H. Cui, J.-Y. Wang, M.-Q. Hu, C.-B. Ma, H.-M. Wen, X.-W. Song and C.-N. Chen, *Dalton Trans.*, 2013, **42**, 8684-8691; (c) D. Yang, Y. Li, B. Wang, X. Zhao, L. Su, S. Chen, P. Tong, Y. Luo and J. Qu, *Inorg. Chem.*, 2015, **54**, 10243-10249; (d) D. Yang, Y. Li, L. Su, B. Wang and J. Qu, *Eur. J. Inorg. Chem.*, 2015, 2965-2973; (e) P. Tong, W. Xie, D. Yang, B. Wang, X. Ji, J. Li and J. Qu, *Dalton Trans.*, 2016, **45**, 18559-18565.
- 32 (a) M. Rakowski DuBois and D. L. DuBois, *Chem. Soc. Rev.*, 2009, **38**, 62-72; (b) T. B. Rauchfuss, *Acc. Chem. Res.*, 2015, **48**, 2107-2116; (c) M. E. Ahmed, S. Dey, M. Y. Darensbourg and A. Dey, *J. Am. Chem. Soc.*, 2018, **140**, 12457-12468.
- 33 G. M. Sheldrick, *SADABS, Program for area detector adsorption correction*, Institute for Inorganic Chemistry, University of Göttingen, Germany, 1996.
- 34 (a) G. M. Sheldrick, *SHELXL-97, Program for refinement of crystal structures*, University of Göttingen, Germany, 1997; (b) G. M. Sheldrick, *SHELXS-97, Program for solution of crystal structures*, University of Göttingen, Germany, 1997.

A table of content entry



A bioinspired thiolate-bridged dinickel complex featuring a pendant amine realizes electrocatalytic hydrogen evolution at a relatively low overpotential.